Magneto-optical study on exciton screening in p-type $Al_xGa_{1-x}As/In_yGa_{1-y}As$ quantum wells

M. Kemerink and P. M. Koenraad
COBRA Interuniversity Research Institute, Eindhoven University of Technology, P.O. Box 513, 5600 MB Eindhoven, The Netherlands

P. C. M. Christianen
Research Institute for Materials, High Field Magnet Laboratory, University of Nijmegen, Toernooiveld, NL-6525 ED, Nijmegen, The Netherlands

R. van Schaijk*
COBRA Interuniversity Research Institute, Eindhoven University of Technology, P.O. Box 513, 5600 MB Eindhoven, The Netherlands

J. C. Maan
Research Institute for Materials, High Field Magnet Laboratory, University of Nijmegen, Toernooiveld, NL-6525 ED, Nijmegen, The Netherlands

J. H. Wolter
COBRA Interuniversity Research Institute, Eindhoven University of Technology, P.O. Box 513, 5600 MB Eindhoven, The Netherlands
(Received 20 January 1997)

We have studied exciton unbinding in empty and p-doped quantum wells, using magnetophotoluminescence excitation measurements. The use of p-type quantum wells allows us to discriminate unambiguously between exciton bleaching by Coulomb screening and by the Pauli exclusion principle. We found that the ground-state heavy-hole exciton, which experiences both effects, is unbound at hole densities in the range $(6-9)\times10^{15}$ m^{-2}. In contrast, the ground-state light-hole and first excited heavy-hole excitons, which are only screened by the Coulomb interaction, still have a finite binding energy at these densities. However, for both bands, its value is far below what is found in an undoped well. Furthermore, we found a strong indication that, in p-doped wells, the excitons of excited subbands are less efficiently screened than those of the light-hole ground state, due to the lesser overlap of the screening ground-state heavy holes with the excited subbands than with the ground-state light holes. [S0163-1829(97)07732-1]

I. INTRODUCTION

The unbinding or bleaching of excitons in semiconductor heterostructures has been the subject of numerous investigations during the past decade. Theoretically, exciton unbinding by interaction with either a sea of a single type of free carriers,[1–4] or photocreated carriers or excitons[5,6] has been considered. Usually, a distinction is made between Coulomb screening and bleaching mechanisms that are related to the Pauli exclusion principle, i.e., phase-space filling and exchange. Qualitatively, Coulomb screening can be thought of as a rearrangement of free carriers in the presence of a disturbing electrostatic potential, e.g., of a photocreated electron or hole, which compensates the disturbing potential. Bleaching mechanisms that are due to the exclusion principle are based on the fermion character of electrons and holes: once a state is occupied by a particle, free or bound, it cannot be used to form an exciton. This mechanism is usually referred to as phase-space filling. Furthermore, the presence of other electrons or holes leads to a modification of the electron-hole interaction, which results in an enhancement of the exciton radius and hence a reduction of its binding energy, which mechanism is generally referred to as exchange. It is important to note that Coulomb screening affects excitons of all subbands, whereas, the other mechanisms are restricted to occupied subbands.

In experiments on exciton bleaching by photocreated free carriers or excitons contradictory results have been obtained regarding the relative importance of Coulomb screening and effects of the Pauli exclusion principle.[7–11] Furthermore, the bleaching effectiveness of various states of the photogenerated carriers, i.e., hot or cold plasma or excitons, seems to be a source of disagreement between theory and experiment.[10–12] The study of exciton bleaching by a single type of carrier circumvents the latter problem, whereas the former question concerning the relative importances of Coulomb screening and Pauli effects can be addressed by using p-type doping, since it allows us to discriminate unambiguously between them, as will be shown below. Most authors dealing experimentally with exciton unbinding in doped systems have only shown qualitative effects.[13–16] In particular, peaks in optical-absorption spectra are usually taken as an indication for the presence of excitons. This method can be misleading due to the presence of Van Hove singularities[17] or due to carrier-induced broadening of absorption peaks.[18]

In this paper, we will quantify the effects of a sea of free heavy holes on the exciton binding energy of various subbands in GaAs and $In_xGa_{1-x}As$ quantum wells (QWs). We will show that excitons of occupied subbands are fully unbound at hole densities in the range $(6-9)\times10^{15}$ m^{-2}. Excitons of unoccupied subbands, in contrast, will be shown to have a finite binding energy at these densities. However, its

value is far below what is found in an undoped well. Furthermore, it seems likely that, in p-doped wells, the excitons of excited subbands are less efficiently screened than those of the light-hole ground state, due to the lesser overlap of the screening ground-state heavy holes with the excited subbands than with the ground-state light holes.

The remainder of this paper will be organized as follows. In Sec. II we will outline the model that was used to interpret the magnetoabsorption spectra that are presented in Sec. III. The data will be discussed in Sec. IV. Section V will summarize our conclusions.

II. THEORETICAL

The total Hamiltonian describing the relative motion of an electron-hole pair in a confining electrostatic potential can in general be written as $H_{ex}=T_h+T_e+U_{e\text{-}h}+U_v+U_c$. The first two terms on the right-hand side describe the kinetic energy of the hole and electron, respectively. The third term describes the screened Coulomb interaction and the last two terms describe the confining potentials of the valence and conduction band, respectively. The corresponding eigenvalue problem has been solved by Bauer and Ando[19] and Yang and Sham[20] for a quantum-well potential in a perpendicular magnetic field. This is, however, an extremely laborious and far from trivial task. Therefore we simplify the problem by solving the hole and electron Hamiltonians, with inclusion of their respective electrostatic potentials $U_{v,c}$, separately, as a function of magnetic field, and correct for the exciton binding energy afterwards. A *posteriori* exciton corrections to free Landau levels have already successfully been used in the high-field limit.[21,22] The price paid for this simplification consists mainly of the fact that anticrossings between excitonic states that are coupled by the Coulomb interaction cannot be reproduced. Despite this, the calculated exciton energies will be shown to match experimental data closely, except in the vicinity of apparent anticrossings.

The hole Landau levels are calculated from the 4×4 Luttinger Hamiltonian on the basis $m_{Jz}=(\frac{3}{2},-\frac{1}{2},\frac{1}{2},-\frac{3}{2})$. The magnetic field B is assumed to be parallel to the quantization axis z, i.e., perpendicular to the plane of the QW. Starting from the matrix expression for $B=0$,[23,24] we follow the usual procedure[25] of replacing k_x and k_y by their operator expressions, written in terms of the standard raising and lowering operators. Making the eigenvector ansatz[25]

$$\Psi_N=(\phi_N^{h+}(z)U_{N-2},\phi_N^{I-}(z)U_N,\phi_N^{I+}(z)\times U_{N-1},\phi_N^{h-}(z)U_{N+1}), \tag{1}$$

where the U_N are the harmonic-oscillator eigenfunctions, we arrive at the following Hamiltonian:

$$\underline{H_N}=\frac{\hbar^2}{m_0}\begin{bmatrix} \frac{\gamma_1+\gamma_2}{R_c^2}\frac{2N-3}{2}+(\gamma_1-2\gamma_2)k_z^2 & -\frac{\sqrt{3}}{R_c^2}\gamma\sqrt{(N-1)N} & -\frac{\sqrt{6}}{R_c}\gamma_3\sqrt{N-1}k_z & 0 \\ -\frac{\sqrt{3}}{R_c^2}\gamma\sqrt{(N-1)N} & \frac{\gamma_1-\gamma_2}{R_c^2}\frac{2N+1}{2}+(\gamma_1+2\gamma_2)k_z^2 & 0 & \frac{\sqrt{6}}{R_c}\gamma_3\sqrt{N+1}k_z \\ -\frac{\sqrt{6}}{R_c}\gamma_3\sqrt{N-1}k_z & 0 & \frac{\gamma_1-\gamma_2}{R_c^2}\frac{2N-1}{2}+(\gamma_1+2\gamma_2)k_z^2 & -\frac{\sqrt{3}}{R_c^2}\gamma\sqrt{(N+1)N} \\ 0 & \frac{\sqrt{6}}{R_c}\gamma_3\sqrt{N+1}k_z & -\frac{\sqrt{3}}{R_c^2}\gamma\sqrt{(N+1)N} & \frac{\gamma_1+\gamma_2}{R_c^2}\frac{2N+3}{2}+(\gamma_1-2\gamma_2)k_z^2 \end{bmatrix}, \tag{2}$$

where R_c is the classical cyclotron orbit $(\hbar/eB)^{1/2}$. We have neglected the bandwarping by taking $\gamma_3-\gamma_2=0$ and $\gamma=(\gamma_2+\gamma_3)/2$. Since $U_i=0$ for $i<0$, the corresponding elements in Eq. (2) should be set to zero, and Eq. (2) is reduced to 3×3, 2×2, 1×1 for $N=1$, 0, −1, respectively. The total eigenvalue equation for the holes now becomes

$$\left[\underline{H_N}+\left(\frac{\hbar^2\kappa}{R_c^2m_0}\left(\frac{3}{2},-\frac{1}{2},\frac{1}{2},-\frac{3}{2}\right)+(U_{v,h}(z),U_{v,l}(z),U_{v,l},(z),U_{v,h}(z))\right)\cdot\underline{I_4}\right]\Psi_N=E_N\Psi_N, \tag{3}$$

where $\underline{I_4}$ in the 4×4 unit matrix and $U_{v,h}(z)$ and $U_{v,l}(z)$ are the strain-dependent valence-band potentials for heavy and light holes, respectively, which also contain the electrostatic potentials of the charged acceptors and the free holes. The second term in Eq. (3), in which κ is the hole g factor, describes the Zeeman splitting of the holes.

Equation (3) is solved numerically, by the method outlined in an earlier publication.[24] This method is numerically exact but requires that Eq. (3) is transformed into a set of coupled first-order real differential equations.[26] Since Eq. (3) is second order and complex, this would yield 16 equations, plus two for normalization and energy continuity. We found by observation that Ψ_N can be decoupled in two independent spinors, that both contain the same information as Ψ_N. The two spinors are

$$\Psi_N^{(I)}=\begin{pmatrix} i\ \mathrm{Im}(\phi_N^{h+}(z))U_{N-2} \\ i\ \mathrm{Im}(\phi_N^{I-}(z))U_N \\ \mathrm{Re}(\phi_N^{I+}(z))U_{N-1} \\ \mathrm{Re}(\phi_N^{h-}(z))U_{N+1} \end{pmatrix},$$

TABLE I. Parameters used in the numerical calculations. Where possible, low-temperature (4.2 K) values are taken. For ternary compounds linear interpolation is used. The parameters are taken from Ref. 46, band gaps from Refs. 47 and 48.

	GaAs	AlAs	InAs
γ_1	6.85	3.45	20.4
γ_2	2.1	0.68	8.3
γ_3	2.9	1.29	9.1
κ	1.2	0.12	7.68
ϵ_r	12.79	10.00	15.15
m_{el}^*	0.067	0.150	0.0239
Δ_{SO} (meV)	340	280	380
$Eg(Al_xGa_{1-x}As)$	$1519.2+1360x+220x^2$ (meV)		
$Eg(In_yGa_{1-y}As)$	$1519.2-1583.7y+475y^2$ (meV)		

$$\Psi_N^{(I)}=\begin{pmatrix} \mathrm{Re}(\phi_N^{h+}(z))U_{N-2} \\ \mathrm{Re}(\phi_N^{I-}(z))U_N \\ i\ \mathrm{Im}(\phi_N^{I+}(z))U_{N-1} \\ i\ \mathrm{Im}(\phi_N^{h-}(z))U_{N+1} \end{pmatrix}, \quad \Psi_N=\Psi_N^{(I)}+\Psi_N^{(II)}, \tag{4}$$

Re( ) and Im( ) denote the real and imaginary parts of the expression between brackets, respectively. Since any linear combination of these two spinors is a solution to Eq. (3), we can set one of these to zero, without changing the eigenvalue. By doing so, the number of first-order differential equations is reduced to 10. This set of equations is solved together with the Poisson equation to ensure self-consistency of the wave functions and electrostatic potentials. The parameters used in the calculations are listed in Table I.

Electron eigenvalues and eigenfunctions are calculated from the standard one-dimensional (1D) Schrödinger equation, and corrected for nonparabolicity[27] by the expression $E_N=E(N,B,k_z)[1+(K_2/E_g)^*E(N,B,k_z)]$, where $E(N,B,k_z)$ is the expectation value of the kinetic energy of the electron. The nonparabolicity parameter K_2 is calculated with the expression derived by Lindemann *et al.*[28] For GaAs and $In_{0.10}Ga_{0.90}As$ one obtains $K_2=-0.83$ and -0.81, respectively, using the parameters given in Table I.

The strain-dependent potentials $U_{v,h}$ and $U_{v,l}$ in Eq. (3) are calculated within the framework of the model-solid theory of Van de Walle.[29] Deformation potentials and elastic moduli are also taken from Ref. 29. For the band offset ratio of unstrained $GaAs/Al_xGa_{1-x}As$, for which material system reliable experimental data are available, we used the commonly accepted value of 0.7/0.3.

The exciton binding energy E_b was modeled using a modified version of the 2D hydrogen model described by MacDonald and Ritchie:[30]

$$E_b(n,\gamma)=E_{2\text{D-}H}(n,m=0,\gamma)-\gamma(2n+1)\ \ \mathrm{Ry_{scale}}. \tag{5}$$

In Eq. (5), $\gamma\equiv\hbar\omega_c/2\ \mathrm{Ry_{scale}}$, with $\mathrm{Ry_{scale}}$ the exciton effective Rydberg, which is used as a scaling parameter, and $\omega_c=eB/\mu^*\cdot\mu^*$ is the effective exciton mass, $(1/m_e^*+1/m_h^*)^{-1}$, with m_e^* and m_h^* the effective in-plane electron and hole masses, respectively. $E_{2\text{D}-H}(n,m=0,\gamma)$ is the energy of a two-dimensional n-s exciton with a zero-field binding energy of 4 $\mathrm{Ry_{scale}}$. In Ref. 30, $\mathrm{Ry_{scale}}$ is equal to the *bulk* Rydberg, Ry*. In the high-field regime ($\gamma\gg1$) Eq. (5) reduces, for the $1s$ exciton ($n=0$), to

$$E_b(B,\mathrm{Ry_{scale}})=-\left[\pi\ \ Ry_{\mathrm{scale}}\frac{\hbar eB}{\mu^*}\right]^{1/2}. \tag{6}$$

The effects of dimensionality and screening are accounted for by using $\mathrm{Ry_{scale}}$ as a free parameter. This scaling is essentially different from the one used in Refs. 21 and 22, where the high-field 2D result from Akimoto and Hasegawa[31] is scaled with a dimensionality parameter D_1, with $D_1=1$ ($\frac{1}{4}$) for two, (three) dimensions:

$$E_b(n,B,\mathrm{Ry^*})=-3D_1\ \ \mathrm{Ry^*}\left[\frac{\hbar eB}{2(2n+1)\mu^*\mathrm{Ry^*}}\right]^{1/2}. \tag{7}$$

The zero-field binding energy becomes $4D_1$ Ry*. It is obvious that Eqs. (6) and (7) are mathematically equivalent, apart from a constant factor. As a result, different exciton binding energies will be found when experimental data are fitted with either Eqs. (6) or (7). We will come back to this in Sec. III.

The question remains how Eq. (5) should be scaled in arbitrary magnetic fields, i.e., whether a dimensionality prefactor, as in Eq. (7), should be used, or if the effective Rydberg should be scaled, as in Eq. (6). Belle[32] has shown that the exact 2D result is a very close approximation to the adiabatic[33] 3D result. The premise to this equality is that, in both limits, the magnetic field and energies are scaled as $\hbar\omega_c/\mathrm{Ry_{scale}}$ ($=2\gamma$) and $E/\mathrm{Ry_{scale}}$, respectively. $\mathrm{Ry_{scale}}$ should be taken as Ry* in the 3D limit and 4 Ry* in the 2D limit. As a consequence, the proper way to scale Eq. (5) is to scale the effective Rydberg $\mathrm{Ry_{scale}}$.

It is worthwhile to point out that the basic assumption of our model is the following. Although it is known that the valence-band nonparabolicity strongly effects the size of the exciton binding energy,[3,34] the effect of nonparabolicity on its field dependence will probably be much smaller. The former effect can simply be compensated by adopting the appropriate value of $\mathrm{Ry_{scale}}$, which is the only free parameter in our description of the field dependence of energy levels.

In the above we have proposed that the dimensionality of the exciton can be accounted for by scaling the effective Rydberg. It is, however, not obvious that the effects of screening and band filling on the exciton energy and its field dependence can be caught by such a simple scaling. For

example, Henriques *et al.* have shown that the Coulomb screening of an exciton in an unoccupied subband is strongly reduced in high magnetic fields due to the shrinkage of the exciton wave function.[35] In Sec. III we will show experimentally that screened excitons can also be described by this ''scaled hydrogen model.''

III. EXPERIMENT

A. Samples and setup

In this study, we will present results from two p-doped $Al_xGa_{1-x}As/In_yGa_{1-y}As$ single-quantum wells (SQW's), with nominal indium concentrations of 0% and 10% and one undoped $GaAs/Al_xGa_{1-x}As$ 10-period multiple quantum well (MQW's) structure. All samples were grown by conventional molecular beam epitaxy (MBE) techniques on ⟨100⟩-oriented GaAs substrates and were grown in different runs of the MBE machine. The p-doped samples consist of a single quantum well, separated by a thin buffer layer from a short period superlattice. Both wells are nominally 95 Å wide, and symmetrically doped with Be δ layers, which are separated from the well by 250 Å spacer layers. The GaAs well is confined by $Al_{0.45}Ga_{0.55}As$ barriers and grown at 690 °C. The $In_{0.10}Ga_{0.90}As$ well is confined by $Al_{0.25}Ga_{0.75}As$ barriers and grown at 500 °C to avoid indium diffusion. The MQW's sample consists, nominally, of ten periods of a 100 Å GaAs SQW confined by 500 Å $Al_{0.33}Ga_{0.67}As$ barriers. Each period was separated from its neighbors by 100 Å AlAs layers. The whole MQW was grown at 800 °C, on top of a short period superlattice. All samples are capped by a 170 Å GaAs layer.

The MQW sample was characterized by high-resolution roentgen diffraction measurements. The well width was found to be 80 ± 2 Å and the Al content of the confining barriers was found to be (36 ± 1)%. X-ray diffraction spectra of the single QW samples turned out to be hardly affected by the actual parameters of the single well. This is due to the relative narrowness of the single well, compared to the thickness of the total structure. The carrier densities, as obtained by transport measurements at 1.4 K, are $(9.0\pm0.1)\times10^{+15}$ and $(6.0\pm0.1)\times10^{+15}$ m^{-2} for the GaAs and $In_xGa_{1-x}As$ SQW samples, respectively. Transport mobilities for both samples are typically around 10 m^2/V s.

The magnetophotoluminescence and photoluminescence excitation (PL, PLE) spectra were measured at 4.2 K. The samples were excited using normal incident light from a tunable Ti:sapphire laser, pumped by an argon-ion laser. In order to assure that the optical spectra were not influenced by heating effects, care was taken that no change in the spectra occurred upon a decrease of excitation power. All experiments were performed in the Faraday configuration, using circular polarized light in excitation as well as in detection. This allows us to separate the light- and heavy-hole components to the total absorption by using either cross (σ^{+-} or σ^{-+}) or parallel (σ^{++} or σ^{--}) polarizations.[36]

Part of the zero and low-field measurements were performed in a different setup, which was described in an earlier publication.[17] Some PL(E) results on the single QW samples were also presented in this publication.

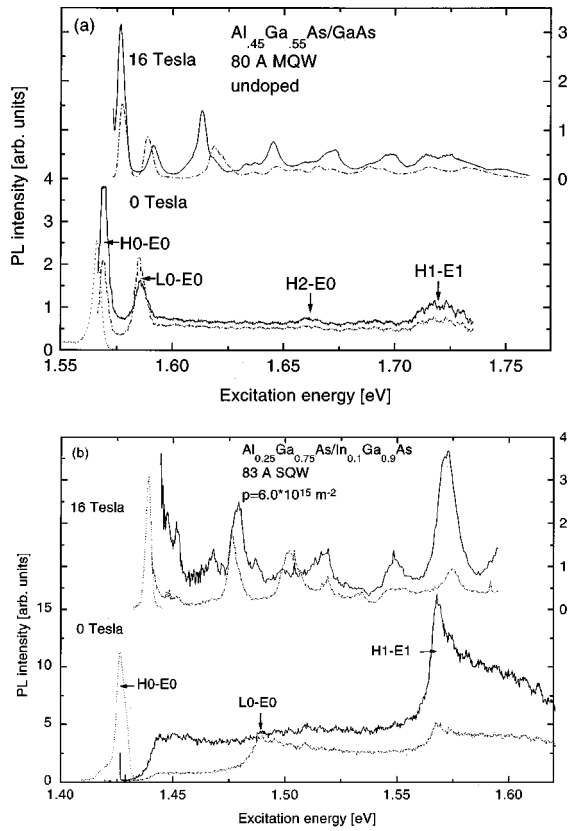

FIG. 1. Low-temperature (4.2 K) PL and PLE spectra at 0 and 16 T for the undoped GaAs MQW (a) and the doped $In_xGa_{1-x}As$ SQW (b). Solid (dash-dotted) lines denote PLE spectra in σ^- (σ^{+-}) polarization. The dotted lines are PL spectra.

B. Experimental results

In Fig. 1(a) raw PLE spectra of the undoped GaAs MQW sample are shown for zero and high magnetic field. In the zero-field traces the strong absorption peaks of the $H0$-$E0$ and $L0$-$E0$ excitons, at 1.57 and 1.59 eV, are clearly visible. [In our notation Hi (Li) stands for a heavy- (light-) hole state with quantum number i, e.g., $H0$ is the heavy-hole ground state, and $H1$ the first excited heavy level.] Their relatively large full width at half maximum (FWHM) is the result of well width variations in the 10-period MQW structure. This also explains the absence of sharp absorption peaks for the $H1$-$E1$ (at 1.72 eV) and $H2$-$E0$ (at 1.66 eV) excitons. Since the binding energies of these excited subbands are more sensitive to well width fluctuations than those of the ground states, the exciton absorption peak is also much stronger smeared out for these higher subbands. In the following, we will show that these transitions still are of excitonic nature, although the corresponding enhancement of oscillator strength is blurred. The 16-T PLE traces in Fig. 1(a) show pronounced, but again broadened, Landau levels.

The zero-field PLE spectra of both doped SQW's qualitatively differ from the ones of the undoped MQW. In Fig. 1(b) this is illustrated by the spectra of the $In_xGa_{1-x}As$ SQW. Both the $H0$-$E0$ and $L0$-$E0$ absorption onsets lack the excitonic enhancement that is present in the spectra of Fig. 1(a), whereas the $H1$-$E1$ onset still shows excitonic effects. This already suggests that the Coulomb screening by the sea of free ($H0$) holes is more efficient for the $L0$-$E0$

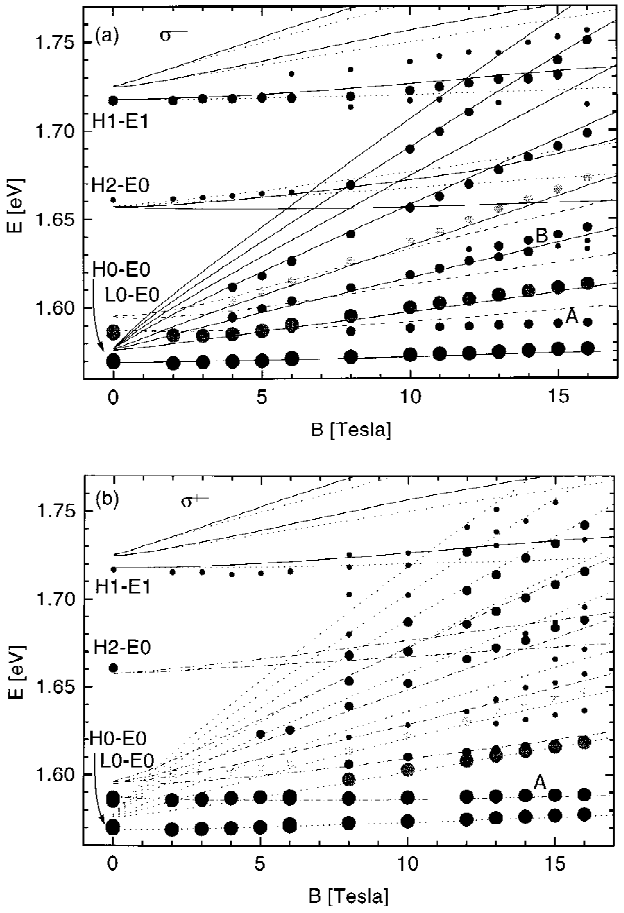

FIG. 2. Magnetic-field dependence of PLE maxima of the undoped GaAs MQW, observed in σ^{--} (a) and σ^{+-} (b) polarization. The size of the dots is indicative of the absorption strength. The lines are calculations, using the model outlined in the text. Solid (dotted) lines denote $H\uparrow$ $(H\downarrow)$ to $E\uparrow$ $(E\downarrow)$ transitions. Dashed (dash-dotted) lines denote $L\uparrow$ $(L\downarrow)$ to $E\uparrow$ $(E\downarrow)$ transitions. For clarity, in the ground states only those transitions are depicted that, at $k=0$ and $B=0$, can be excited by the incoming light, according to the selection rules for circular polarized light.

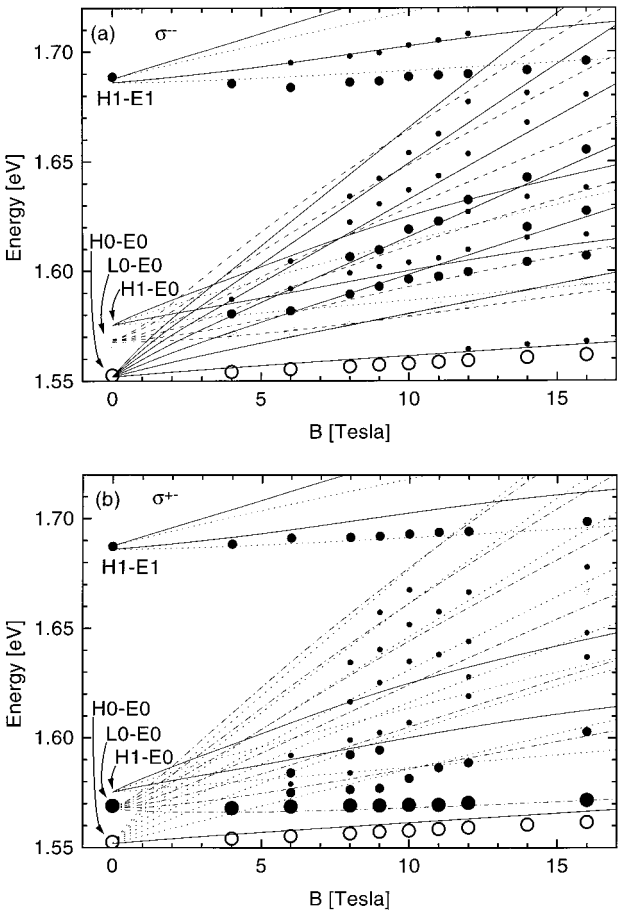

FIG. 3. Same as Fig. 3, for the doped GaAs SQW. The open symbols are taken from PL maxima instead of PLE.

exciton than for the $H1$-$E1$ exciton. Note that enhancement of the $H1$-$E1$ absorption onset cannot be due to a second-order van Hove singularity, since the $H1$ mass differs significantly from the electron mass.[17]

The summary of all magneto-PL(E) measurements in two polarization configurations is displayed by the dots in Figs. 2–4. The size of the dots is indicative of the strength of the absorption. Error bars are typically of the size of the smallest dots (1–2 meV), except for the $H2$-$E0$ and $H1$-$E1$ transitions in the undoped GaAs MQW and for the $H1$-$E1$ transition in the doped GaAs SQW where the error bar is approximately the size of the intermediate dot (4 meV). The lowest lines of the doped QW's are taken from emission (PL) spectra, since absorption (PLE) is prohibited by the occupation of the lowest Landau levels. Being due to emission, the detected PL line is selected by the detection polarization, in contrast with the PLE lines, which are selected by the excitation polarization.

The lines in Figs. 2–4 are calculated using the model outlined in the previous section. The parameters used in the calculations are listed in Table II. In the numerical calculations, the well width and, for the doped samples, the band-gap renormalization (BGR) were used as free parameters. The BGR was incorporated as a rigid shift of all bands. Recent local-density approximation (LDA) calculations, in which the complications due to the coexistence of both heavy and light holes were taken into account, proved this assumption to be justified within a few meV.[37] Therefore, the well width was fully determined by the energetic separation between the $H0$-$E0$, $L0$-$E0$, and $H1$-$E1$ transition onsets, which were corrected for their respective exciton binding energies. These exciton binding energies, in turn, were obtained by minimizing the difference in magnetic-field dependence of the calculated and measured transition energies. The total procedure is, of course, a sort of self-consistency problem, which was solved by iteration. Fortunately, the calculated free Landau levels hardly depend on small changes in well width, which effectively makes the exciton binding energy the only free parameter in describing the field dependence of the various levels. For the MQW, the well dimensions could also be obtained from high-resolution x-ray-diffraction measurements. The value found was 80 ± 2 Å for both methods. The BGR that was found for the GaAs SQW was 17 ± 2 meV, where the calculations[37] gave 20 meV.

The effective hole mass, needed in Eq. (5) for the calculation of the field dependence of the exciton binding energy, was taken as the average mass of the lowest calculated Landau level, in the field range from 0–20 T, $m_{\mathrm{av}} = 1/2\hbar e\Delta B/\Delta E$. The used values are given in Table II.

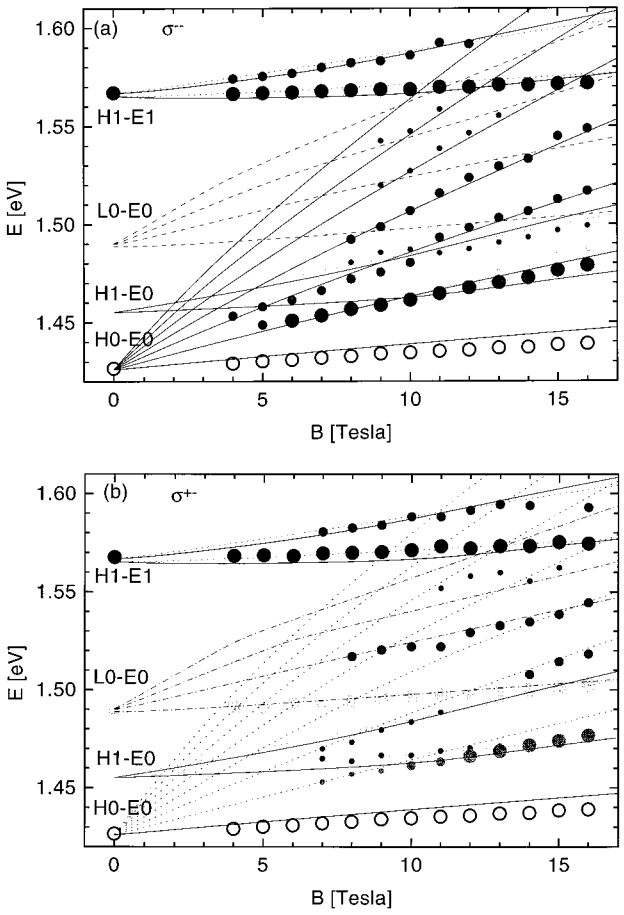

FIG. 4. Same as Fig. 3, for the doped $In_xGa_{1-x}As$ SQW. The open symbols are taken from PL maxima instead of PLE.

These masses are only meant to characterize the lowest Landan level (LL) of each subband and should not be confused with the effective mass at the Fermi level, which is obtained by, e.g., temperature-dependent Shubnikov–de Haas measurements. It should be noted that the field dependence of the exciton binding energy is hardly dependent on the hole mass used in Eq. (5). For a zero-field $1s$ binding energy of 10 meV and an electron mass of $0.067m_0$ the binding energy at 20 T is 22.6 meV for a hole mass of $0.3m_0$ and 21.8 meV for a hole mass of $0.6m_0$. For higher excitons the difference is even smaller.

IV. DISCUSSION

A. Spectral features

The general agreement between the observed and calculated magneto-optical fan charts, as depicted in Figs. 2–4, is apparent. Several features, however, are worth some further discussion.

First, as was indicated in Sec. II A, our model does not account for anticrossings that result from the Coulomb interaction between different excitons. In situations where the anticrossing is abrupt, i.e., has a small anticrossing gap, this is not troublesome for the present purposes. This can, for example, be illustrated by the level marked A in Fig. 2(b), which is the $L0\downarrow$-$E0\uparrow$ $1s$ exciton. Although Bauer and Ando[19] have shown that this state [$l_1(1s)$ in their notation] experiences a sharp anticrossing—with $h_1(3d)$—in the low-field region, the state that is optically active follows the field dependence of the nonanticrossing $L0\downarrow$-$E0\uparrow$ $1s$ exciton. Only in very narrow QW's, where this anticrossing gap is much larger, the actual anticrossing can be resolved.[38] A situation in which our model fails can be found in Fig. 2(a), at the level marked B. Here an anticrossing with, probably, a $H1$-$E0$ state is observed. This anticrossing was also observed by Rogers *et al.*[22] Such a ''missed anticrossing'' might also explain the deviation between calculation and experiment at A in Fig. 2(a). In this polarization (σ^-) the low-field anticrossing between $l_1(1s)$ and $h_1(3d)$ is far less abrupt then in σ^+ polarization.[19] This enhances the magnetic-field region where the anticrossing levels deviate from the nonanticrossing ones, which could cause the deviation of our model from the experimental points. For the degenerate samples, ''missed anticrossings'' are irrelevant since the Coulomb interactions involved are much smaller due to the screening by the free holes.

Second, in the doped SQW's only Landau levels that are above or at the Fermi energy are visible in absorption. As an example, the filling factor of the $In_xGa_{1-x}As$ SQW is 6 at 4.1 T and 4 at 6.2 T, which corresponds quite closely to the visibility onsets of the corresponding $H0$-$E0$ absorption lines in Fig. 4(a). The lowest $H0$-$E0$ transition is, due to the phase-space filling, only visible in PL. At the highest magnetic fields a small, additional peak arises in the PLE spectra, a few meV above the PL line, see Figs. 3(a) and 3(b).[39] We attribute this to absorption in the high-energy tail of the lowest $H0$, $\uparrow$ and $\downarrow$ Landau levels. Therefore, these points should lay above the calculated transition energies. The PL energies

TABLE II. Exciton binding energies, well widths, and hole effective masses used in the calculations for Figs. 3–5 (see text).

	Binding energy (meV)			Width	Hole masses		
	H0-E0	$L0$-$E0$	$H1$-$E1$	(Å)	$H0$	$L0$	$H1$
GaAs MQW	8±1	9±1	8±2	80±2	↑:0.46	↑:0.063	↑:0.045
undoped					↓:0.19	↓:−0.19	↓:0.19
GaAs SQW	0	1±1	2±1	89±2	↑:0.43	↑:0.061	↑:0.042
$p=9\times10^{15}$ m^{-2}					↓:0.19	↓:−0.19	↓:0.19
$In_xGa_{1-x}As$ SQW	0	1±1	2±1	83±2	↑:0.10	↑:0.083	↑:0.15
$p=6\times10^{15}$ m^{-2}					↓:0.19	↓:0.14	↓:0.19

are redshifted with respect to the calculated energies due to the Stokes shift, which results from local variations in the QW properties.

Third, the experimental Landau fans show several transitions that are forbidden by either parity or polarization, when the hole levels are considered parabolic, i.e., when the nondiagonal terms in Eq. (2) are neglected. These transitions can, however, be easily explained by nonparabolicity effects. Ancilotto, Fasolino, and Maan[21] have discussed these effects extensively for an empty SQW, so we will limit ourselves to two illustrative examples. The visibility of the $H1$-$E0$ transition in Figs. 3 and 4 may seem surprising, but it is a direct consequence of admixture in nonzero fields of states with quantum number 0 to the $H1$ state. This change of parity is due to k_z operators in nondiagonal elements of Eq. (2). Admixture of states with the same parity as the original state can explain the observation of transitions that are forbidden by the polarization selection rules. This is the case in Fig. 4(b), were $H0\uparrow$-$E0\uparrow$ is observed in σ^{+-} polarization, due to admixture of $L0\downarrow$ to $H0\uparrow$. We would like to point out that, although the strain in $In_xGa_{1-x}As/GaAs$ QW's enhances the parabolicity of the hole states in the sense that the effective mass remains constant over a wider range of fields and energies, the band mixing cannot be neglected in $In_xGa_{1-x}As$ QW's.

B. Exciton screening

The $H0$-$E0$ transitions in the doped SQW's can be accurately described by setting the exciton binding energy to zero, i.e., setting Ry_{scale} to zero in our model. This is in agreement with both theoretical[1,3] calculations and other experimental work.[40] It could be suggested that the increase in field of the energetic separation between the PL line and the calculated lowest Landau level is an indication that a finite binding energy still exists for the $H0$-$E0$ exciton. There are, however, several arguments against this hypothesis. First, all higher Landau levels that are observed in absorption instead of emission seem to lie at the correct energies. Second, the small absorption peaks just above the PL lines are in accordance with the calculations, as argued above. Furthermore, Gravier *et al.*[41] experimentally observe, for a similar *p*-doped SQW, that the difference between the Stokes shifted PL line and the lowest PLE line increases with magnetic field. Since PLE lines are generally regarded as a correct measure for the ''true'' transition energy, the observation by Gravier *et al.* supports our argument.

For the $L0$-$E0$ and $H1$-$E1$ transitions, the correspondence between measurement and calculation is significantly better when a finite exciton binding energy is used than when it is omitted. This shows that a finite exciton binding energy remains present up to very high free-carrier concentrations when the screening is purely of Coulombic nature. This is a very strong confirmation of various theoretical works in which it was argued that 2D Coulomb screening cannot fully destroy the exciton binding energy, and one bound state remains at all densities.[1,3,42] However, the conclusion of Ref. 9 that ''intersubband effects via Coulomb screening are negligible'' in modulation doped QW's seems unjustified. The fact that, in the doped wells, a smaller binding energy is found for the $L0$-$E0$ exciton than for the $H1$-$E0$ exciton is in good qualitative agreement with the zero-field absorption spectra. As can been seen from Fig. 1(b), an excitonic enhancement of the $L0$-$E0$ absorption is fully absent, whereas it is clearly present for $H1$-$E1$.

The extremely small binding energy that is obtained for the $L0$-$E0$ excitons (1 ± 1 meV) is in good agreement with the results of Refs. 1 and 3 who find 0.2 and 0.5 meV, respectively. In contrast, the $H1$-$E1$ binding energy seems to be underestimated in the calculations of Ref. 3 by almost its full value: we find 2 ± 1 meV, versus (almost) zero in Ref. 3. This discrepancy is probably due to the purely 2D model in which the screening was calculated. Although the finite extent of the screening subband, $H0$, in the z direction is taken into account by a form factor, only the average electrostatic potentials of the screened excitons and the average density of the screening subband are used, as was pointed out by Henriques.[4] This leads to a dielectric constant $\epsilon(\mathbf{q})$ that is independent of z. Due to the fact that the $H0$ subband and the $H1$-$E1$ exciton have their maximum charge densities $[\sim|\Psi(z)|^2]$ at different z values, this procedure results in an overestimation of the screening efficiency and hence an underestimation of the exciton binding energy. For the $L0$-$E0$ exciton this effect is of minor importance due to the similarity of the $H0$, $L0$, and $E0$ wave functions. It is important to note that the $In_xGa_{1-x}As$ $H1$-$E1$ exciton binding energy found in this work, 2 ± 1 meV, is consistent with the result from temperature-dependent absorption strength measurements on the same sample, which yielded an E_b between 1.0 and 2.5 meV.[17]

The absence of exciton binding for $H0$-$E0$, and its presence for $L0$-$E0$, shows the effects of occupation, by phase-space filling and exchange, on the exciton bleaching. Since the $H0$ and $L0$ wave functions are almost equal, the effect of Coulomb screening will be almost the same for the $H0$-$E0$ and $L0$-$E0$ excitons, as discussed above. Differences in exciton bleaching between these two subbands therefore, necessarily arise from the difference in occupation. Our results, therefore, also confirm the theoretical claim that no excitonic bound state exists for highly degenerate subbands.

TABLE III. Comparison between exciton binding energies in an undoped GaAs QW, found in the current work and those found by Rogers *et al.* (Ref. 22). All values are in meV. See text for further explanation.

	This work		Rogers *et al.* (Ref. 22)			
	full model	high field	low-field extrapolation		high-field fit	
width	80 Å	80 Å	75 Å	100 Å	75 Å	100 Å
$H0$-$E0$	8 ± 1	10 ± 1	10	8	12 ± 1	$9.5\pm.5$
$L0$-$E0$	9 ± 1	14 ± 1	11	9		

C. Comparison with other models

When we compare the exciton binding energies for the undoped MQW (Table II) with those found by other authors for similar QW's—see e.g, Fig. 4 in Ref. 43 for a summary of various experimental results—it appears that our values for the $H0$ and $L0$ excitons are about 2 meV below the average for 80 Å QW's. The $H0$ binding energy is, however, still somewhat above the value reported by Ossau *et al.*,[44] who determined E_b from the diamagnetic shift of the $H0$ exciton. A comparison with the results of Rogers *et al.*,[22] who determined the exciton binding energy of $H0$-$E0$ both from extrapolation of low-field data and from fitting high-field data, can easily be made. The high-field model used in Ref. 22 assumed linear Landau levels, which were corrected for electron nonparabolicity, and for excitonic effects. The latter correction was made using Eq. (7). Since the full expression (5) for E_b reduces to Eq. (6) in high fields, we can convert our E_b's to the binding energies that fitting with Eq. (7) would yield by demanding equality of Eqs. (6) and (7). Table III summarizes all relevant binding energies. It is obvious that our full results compare more favorable with the binding energies obtained by low-field extrapolation, whereas our results using Eq. (7) agree with the corresponding high-field values found by Rogers *et al.* Although the latter values are somewhat closer to the values reported in Ref. 43, we stick to our original values since we doubt the scaling used in Eq. (7), for reasons pointed out in Sec. II. The $H1$-$E1$ binding energy of 8 meV seems to be in reasonable agreement with the theoretical results of Refs. 34 and 3 who report 9.2 meV for a 150 Å well with $Al_{0.4}Ga_{0.6}As$ barriers and 6.5 meV for a 100 Å well with $Al_{0.25}Ga_{0.75}As$ barriers, respectively.

As was discussed in the Introduction, various authors have used a model in which the electron-hole pairs are described in terms of a scaled 2D hydrogen model.[38,40,41,45] In our model, this comes down to replacing the exact hole Landau levels by their linear counterparts, and neglecting the electron nonparabolicity. When we fit to our experimental fan charts in this model, we find, for the undoped GaAs MQW, $E_b=8$ meV and $m_{H0}=0.6m_0$ for the $H0$-$E0$ exciton, and $E_b=9$ meV and $m_{L0}=-0.6m_0$ for the $L0$-$E0$ exciton. Considering the extreme nonlinearity of the $L0$ Landau levels it may seem surprising that the $L0$-$E0$ binding energy is found to be the same as when the Luttinger model is used to calculate the hole energies. However, this correspondence reflects the fact that, in undoped QW's, the Coulomb energy fully dominates over the nonlinearities in the light- and heavy-hole Landau levels. Since the lowest $H0$ Landau levels are almost linear, the agreement between the simple and the full model is less surprising in this case. Large deviations are found when the fan charts of the doped GaAs QW are fitted in the 2D hydrogenic model. Here, the exciton binding energy no longer dominates over the Landau level nonlinearities, which makes the approximation of the exact Landau levels by their linear counterparts no longer valid. For the $H0$ we find an effective mass of 0.6. The $L0$-$E0$ could best be fitted with a $L0$ mass of -1.0, and a binding energy in the range of 4–7 meV. This, of course, is in contradiction with theoretical predictions, the result of the Luttinger model, and earlier work on the same sample.[17] It should be pointed out that the agreement with the experimental points is, in all aforementioned cases, far better for our model than for the 2D hydrogen model, particularly for the $L0$-$E0$ transition in the doped GaAs SQW. Due to the strain-enhanced linearity of the hole Landau levels in the $In_xGa_{1-x}As$ system, the 2D hydrogen model works satisfactory for the $In_xGa_{1-x}As$ SQW.

D. Numerical results

The hole Landau levels that are used for the generation of the lines in Figs. 2–4 are shown in Fig. 5. Figure 5(a) displays the fan diagram for the unstrained 80 Å GaAs well,

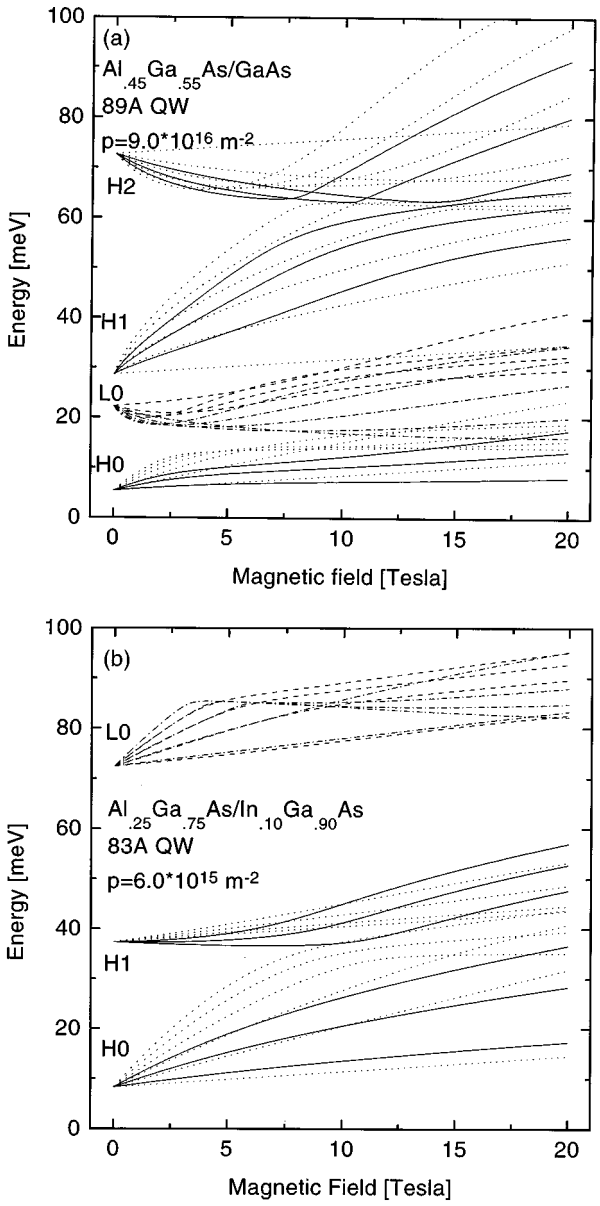

FIG. 5. Valence-band Landau diagrams for (a) an unstrained 89 Å GaAs well, with $Al_{0.45}Ga_{0.55}As$ barriers and a hole concentration of 9.0×10^{15} m^{-2} and (b) a strained 83 Å $In_{0.10}Ga_{0.90}As$ well between $Al_{0.25}Ga_{0.75}As$ barriers, with a hole concentration of 6.0×10^{15} m^{-2}. For clarity, only Landau levels with $N\leqslant4$ are shown. The solid (dotted) lines are $H\uparrow$ ($H\downarrow$) Landau levels, the dashed (dash-dotted) lines denote $L\uparrow$ ($L\downarrow$) levels.

embedded between two $Al_{0.45}Ga_{0.55}As$ barriers, with a hole concentration of 9.0×10^{15} m^{-2}. Figure 5(b) shows the same for the strained 83 Å $In_{0.10}Ga_{0.90}As$ well between $Al_{0.25}Ga_{0.75}As$ barriers, with a hole concentration of 6.0×10^{15} m^{-2}. The doping was assumed to be symmetrically distributed over two δ-layers on the left- and right-hand side of the sample. Due to the axial component of the compressive strain in the $In_xGa_{1-x}As$ QW, the light-hole levels are shifted upward with respect to the heavy-hole levels. The two most striking effects of this shift are the disappearance of the negative $L0$ mass and the decreased $H0$ mass for higher Landau levels. Since the negative $L0$ mass in the GaAs QW is the result of a strong repulsive interaction between $H1$ and $L0$,[21] it changes sign as soon as the $H1$ level drops below $L0$. As this repulsive interaction is still present in the $In_xGa_{1-x}As$ QW, the $H1$ mass is strongly increased compared to the $H1$ mass in the GaAs SQW. The kink in the $L0$ Landau levels at 87 meV, see Fig. 5(b), is due to an anticrossing with the $H2$ state. The disappearance of the negative $LH0$ mass is confirmed by the change in field dependence of the lowest $L0$-$E0$ transition in Figs. 3(b) and 4(b). The decrease of the $H0$ mass, going from GaAs to $In_xGa_{1-x}As$, is also a consequence of the shift in the position of the $L0$ level. Since the extreme bending of the $H0$ Landau levels and its high effective mass are, in the GaAs QW, mainly caused by the anticrossing with the $L0$ level, the ''removal'' of the $L0$ level in the $In_xGa_{1-x}As$ SQW results in a smaller effective mass and a larger range in which the $H0$ Landau levels can be considered as linear.

The hole masses listed in Table II show, on first sight, remarkable constancy for the heavy holes with ''spin'' down ($m_J=-\frac{3}{2}$). For the GaAs wells, this can be understood by realizing that the masses listed are those of the lowest Landau level of each state. For the heavy-hole down state, the lowest Landau level has $N=-1$ and the Hamiltonian (2) is reduced from 4×4 to 1×1. In other words, heavy-hole down states with $N=-1$ do not interact with other states and, consequently, their effective mass only depends on the Luttinger parameters. The constancy of the heavy-hole down mass in going from GaAs to $In_xGa_{1-x}As$ is due to a cancellation of a decreasing in-plane mass [$\propto1/(\gamma_1+\gamma_2)$] and an increasing Zeeman energy[49] [$\propto(-\kappa)$ for ''spin'' down states].

V. CONCLUSION

We have shown that in degenerate p-type samples, both the $L0$-$E0$ and $H1$-$E1$ excitons, which are only screened by the Coulomb interaction with the free ground-state heavy holes, are strongly screened. However, a finite binding energy remains present up to very high free-carrier densities ($6-9\times10^{15}$ m^{-2}), in agreement with 2D screening theory. The $H0$-$E0$ exciton, in contrast, is totally unbound at these densities, due to the combined effects of Coulomb screening and occupation related bleaching. Furthermore, we found strong experimental indications that the usual 2D random-phase approximation screening theory overestimates the screening strength for excited subbands. This is due to neglecting the z dependence in the charge density of various subbands. Due to the similarity of $H0$ and $L0$ wave functions, the screening of the $L0$-$E0$ exciton is, for the studied QW's, predicted correctly by standard 2D screening theory.

We have succesfully used a simplified model to describe the excitonic transitions in III/V heterostructures, which is based upon a separation of the full Hamiltonian into parts, which are solved separately. The extreme nonlinearity of the $H0$ and $L0$ Landau levels can be reduced by incorporating compressive strain in the QW material, as was found from both the experimental and the numerical results. However, for high fields and high Landau indices band mixing remains important, as was confirmed by experimental observations on an $In_{0.10}Ga_{0.90}As$ QW.

ACKNOWLEDGMENTS

We gratefully acknowledge W. C. van der Vleuten for sample growth and C. E. van Es and T. J. Eijkemans for sample characterization and x-ray diffraction measurements. This work is part of the research program of the Stichting voor Fundamenteel Onderzoek der Materie (FOM), which is financially supported by the ''Nederlandse Organisatie voor Wetenschappelijk Onderzoek (NWO).''

*Present and permanent address: Faculty of Mathematics, Computer Science, Physics and Astronomy, University of Amsterdam, Valckenierstraat 65, 1018 XE Amsterdam, The Netherlands.

[1] D. A. Kleinman, Phys. Rev. B **32**, 3766 (1985).
[2] A. E. Ruckenstein and S. Schmitt-Rink, Phys. Rev. B **35**, 7551 (1987).
[3] G. D. Sanders and Y.-C. Chang, Phys. Rev. B **35**, 1300 (1987).
[4] A. B. Henriques, Phys. Rev. B **44**, 3340 (1991).
[5] S. Schmitt-Rink, D. S. Chemla, and D. A. B. Miller, Phys. Rev. B **32**, 6601 (1985).
[6] R. Zimmermann, Phys. Status Solidi B **146**, 371 (1988).
[7] W. H. Knox, C. Hirlimann, D. A. B. Miller, J. Shah, D. S. Chemla, and C. V. Shank, Phys. Rev. Lett. **56**, 1191 (1986).
[8] E. Lach, M. Walther, G. Traenkle, A. Forchel, and G. Weimann, Phys. Status Solidi B **150**, 679 (1988).
[9] K.-H. Schlaad, Ch. Weber, J. Cunningham, C. V. Hoof, G. Borghs, G. Weimann, W. Schlapp, H. Nickel, and C. Klingshirn, Phys. Rev. B **43**, 4268 (1991).
[10] P. C. Becker, D. Lee, A. M. Johnson, A. G. Prosser, R. D. Feldman, R. F. Austin, and R. E. Behringer, Phys. Rev. Lett. **68**, 1876 (1992).
[11] S. Hunsche, K. Leo, H. Kurz, and K. Koehler, Phys. Rev. B **49**, 16 565 (1994).
[12] W. H. Knox, R. L. Fork, M. C. Downer, D. A. B. Miller, D. S. Chemla, C. V. Shank, A. C. Gossard, and W. Wiegmann, Phys. Rev. Lett. **54**, 1306 (1985).
[13] R. C. Miller and D. A. Kleinman, J. Lumin. **30**, 520 (1985).
[14] C. Delalande, G. Bastard, J. Orgonasi, J. A. Brum, H. W. Liu, M. Voos, G. Weimann, and W. Schlapp, Phys. Rev. Lett. **59**, 2690 (1987).
[15] D. Huang, H. Y. Chu, Y. C. Chang, R. Houdre, and H. Morkoc, Phys. Rev. B **38**, 1246 (1988).
[16] H. Yoshimura and H. Sakaki, Phys. Rev. B **39**, 13 024 (1989).
[17] M. Kemerink, P. M. Koenraad, and J. H. Wolter, Phys. Rev. B **54**, 10 644 (1996).
[18] D. R. Wake, H. W. Yoon, J. P. Wolfe, and H. Morkoc, Phys. Rev. B **46**, 13 452 (1992).

[19] G. E. W. Bauer and T. Ando, Phys. Rev. B **38**, 6015 (1988).
[20] S.-R. E. Yang and L. J. Sham, Phys. Rev. Lett. **58**, 2598 (1987).
[21] F. Ancilotto, A. Fasolino, and J. C. Maan, Phys. Rev. B **38**, 1788 (1988).
[22] D. C. Rogers, J. Singleton, R. J. Nicholas, C. T. Foxon, and K. Woodbridge, Phys. Rev. B **34**, 4002 (1986).
[23] D. A. Broido and L. A. Sham, Phys. Rev. B **31**, 888 (1985).
[24] M. Kemerink, P. M. Koenraad, P. C. M. Christianen, A. K. Geim, J. C. Maan, J. H. Wolter, and M. Henini, Phys. Rev. B **53**, 10 000 (1996). Note that a factor 2 was accidentally omitted in the expression for b in Eq. (2) of this publication. The matrix used in the actual calculations was correct.
[25] S.-R. E. Yang, D. A. Broido, and L. J. Sham, Phys. Rev. B **32**, 6630 (1985).
[26] G. Goldoni and A. Fasolino, Phys. Rev. B **51**, 9903 (1995).
[27] E. D. Palik, G. S. Pikus, S. Teitler, and R. F. Wallis, Phys. Rev. **122**, 475 (1971).
[28] G. Lindemann, R. Lassnig, W. Seidebush, and E. Gornik, Phys. Rev. B **28**, 4693 (1983).
[29] C. G. Van de Walle, Phys. Rev. B **39**, 1871 (1989).
[30] A. H. MacDonald and D. S. Ritchie, Phys. Rev. B **33**, 8336 (1986).
[31] O. Akimoto and H. Hasegawa, J. Phys. Soc. Jpn. **22**, 181 (1967).
[32] G. B. Belle, Ph.D. thesis, University of Nijmegen, 1985.
[33] The adiabatic approximation requires that the exciton wave function can practically be decoupled into contributions parallel and perpendicular to the magnetic field. This procedure is only valid if $\gamma \gg 1$.
[34] U. Ekenberg and M. Altarelli, Phys. Rev. B **35**, 7585 (1987).
[35] A. B. Henriques, E. T. R. Chidley, R. J. Nicholas, P. Dawson, and C. T. Foxon, Phys. Rev. B **46**, 4047 (1992).
[36] J. C. Maan, in *Physics and Applications of Quantum Wells and Superlattices*, Vol. 170 of *NATO Advanced Study Institute, Series B: Physics*, edited by E. E. Mendez and K. von Klitzing (Plenum, London, 1987).
[37] P. A. Bobbert, H. Wieldraaijer, R. van der Weide, M. Kemerink, P. M. Koenraad, and J. H. Wolter (unpublished).
[38] M. Potemski, L. Viña, G. E. W. Bauer, J. C. Maan, K. Ploog, and G. Weimann, Phys. Rev. B **43**, 14 707 (1991).
[39] In Figs. 5(a) and 5(b) ($In_xGa_{1-x}As$ SQW) these additional peaks should also be visible. However, these spectra suffer from ''ghost'' lines, which are due to the monochromator and lie very close to the laser energy. This makes a proper analysis of peaks in this energy range impossible.
[40] R. Stepniewski, M. Potemski, H. Buhmann, D. Toet, J. C. Maan, G. Martinez, W. Knap, A. Raymond, and B. Etienne, Phys. Rev. B **50**, 11 895 (1994).
[41] L. Gravier, M. Potemski, A. Fisher, and K. Ploog, Solid-State Electron. **40**, 697 (1996).
[42] J. A. Brum, G. Bastard, and C. Guillemot, Phys. Rev. B **30**, 905 (1984).
[43] E. S. Koteles and J. Y. Chi, Phys. Rev. B **37**, 6332 (1988).
[44] W. Ossau, B. Jäkel, E. Bangert, G. Landwehr, and G. Weimann, Surf. Sci. **174**, 188 (1986).
[45] M. Volk, S. Lutgen, T. Marschner, W. Stolz, E. O. Goebel, P. C. M. Christianen, and J. C. Maan, Phys. Rev. B **52**, 11 096 (1995).
[46] *Physics of Group IV Elements and III-V Compounds*, edited by O. Madelung, M. Schultz, and H. Weiss, Landolt-Börnstein, New Series, Group III, Vol. 17, Pt. a (Springer-Verlag, Berlin, 1982); *ibid.*, Vol. 22, Pt. a (Springer-Verlag, Berlin, 1987).
[47] M. Guzzi and J. L. Steahly, in *Physics of DX Centers in III-V Ternary Compounds*, edited by J. C. Bourgoin (Trans Tech, Aedermannsdorf, 1989).
[48] K. H. Goetz, D. Bimberg, H. Jürgensen, J. Solders, A. V. Solomonov, G. F. Glinskii, and M. Razeghi, J. Appl. Phys. **54**, 4543 (1983).
[49] For electronic Landau levels the Zeeman terms are not included when the effective mass is determined. For hole Landau levels the ''effective mass'' is determined by the interaction with all other subbands. As these subbands in turn also experience a Zeeman energy, there is no consistent way of defining an effective mass without the Zeeman splitting.